

Mass cytometry reveals unique subsets of T cells and lymphoid cells in nasal polyps from patients with chronic rhinosinusitis (CRS)

Kathleen Bartemes¹, Garret Choby¹, Erin O'Brien¹, Janelee Stokken¹, Kevin Pavelko¹, and Hirohito Kita²

¹Mayo Clinic Rochester

²Mayo Clinic Arizona

September 22, 2020

Mass cytometry reveals unique subsets of T cells and lymphoid cells in nasal polyps from patients with chronic rhinosinusitis (CRS)

To the Editor:

Chronic rhinosinusitis (CRS), a heterogeneous disease characterized by chronic inflammation in the nasal cavity and sinuses, causes significant morbidity and diminished quality of life while costing the U.S. health system \$22 to 32 billion annually¹. Aberrant activation of the immune system in nasal and sinus mucosa plays a key role in the etiology and pathophysiology of CRS. Indeed, CRS is associated with increased expression of type 2 and other cytokines in the tissues, and patients have been treated successfully by targeting these molecules². To better understand the pathophysiologic mechanisms of CRS, characterization of the immune cells that infiltrate nasal and sinus tissues is critical. While conventional tools, such as flow cytometry, have been useful for identifying specific immune cell types, the cellular complexity and functional diversity of the human immune system necessitate the use of high-dimensional tools to characterize heterogeneity of immune cells and to elucidate their roles in disease³. Mass cytometry, similar to flow cytometry, is suited to performing single-cell analysis, but with the added advantages of minimal channel overlap and increased multiplexing capacity. Here, we performed a proof of concept pilot study applying mass cytometry to CRS research and characterized the T cell and lymphoid cell populations infiltrating into nasal polyps.

Nasal polyps from 18 subjects with CRS with nasal polyps (CRSwNP) and control sphenoid mucosal tissues from 4 subjects without CRS were obtained (see Supplemental Table E1 for subject demographics). Peripheral blood mononuclear cells (PBMCs) from healthy individuals without sinus disease provided another layer of controls. Tissue cells and PBMCs were stained with selected fluorescent-labeled antibodies or with the mass cytometry metal-labeled T cell panel (Supplemental Table E2). We first compared the performance of both methods using conventional biaxial plots (Supplemental Figure E1). The ratio of CD4⁺ to CD8⁺ cells (Figure 1A) and proportions of CD4⁺, CD8⁺, double-negative (DN), and double-positive (DP) cells within the CD3⁺ T cell compartment (Figure 1B) were similar within each cellular source whether analyzed by flow cytometry or by mass cytometry.

Tissue resident memory T (T_{RM}) cells, which highly express the activation marker and adhesion molecule CD69, likely play a pivotal role in pathophysiology of mucosal organs in immune-mediated diseases⁴. Conventional flow cytometry revealed a significantly greater proportion of CD4⁺ cells co-expressing CD69 in nasal polyps compared to control sinus tissues (Figure 1C, p<0.05); few CD4⁺ T cells in PBMCs expressed CD69. Mass cytometry analysis showed comparable findings. Furthermore, by mass cytometry, both nasal polyps and control tissues contained similar proportions of CD69⁺CD8⁺ T cells (Figure 1D). Overall, by using typical cell surface markers for T cells, such as CD4, CD8 and CD69, mass cytometry analysis roughly

corroborated flow cytometry findings.

To examine T cell subpopulations in nasal polyps more deeply, we analyzed mass cytometry data using supervised and unsupervised data clustering methods via the Astrolabe platform⁵. Supervised clustering utilized the Human ImmunoPhenotyping Consortium hierarchical guidelines⁶ adapted for the conventional markers included in our T cell panel (Supplemental Table E2). Our panel allowed differentiation of 11 T cell subsets (Supplemental Table E3 and Supplemental Figure E2). Supervised clustering identified several significant differences in subset frequencies among nasal polyps, control sinus tissues and PBMCs. For example, both types of tissues contained significantly lower frequencies of naïve CD4⁺ T cells compared to PBMCs (Figure 1E, $p < 0.01$). Similarly, naïve CD8⁺ T cells were significantly less frequent in nasal polyps compared to PBMCs ($p < 0.05$) or control sinus tissues ($p < 0.01$). In contrast, the proportion of CD8⁺ central memory T (T_{CM}) cells was significantly greater in nasal polyps than in control nasal tissue (Figure 1F, $p < 0.01$). Other canonical T cell subsets were not notably different between the two sources of sinus tissues (data not shown).

We next analyzed the mass cytometry data using two methods for unsupervised clustering. A multidimensional scaling (MDS) map of 21 T cell panel markers (Supplemental Table E2) revealed over 77 different cell subsets, including 27 subsets in the CD4⁺ T cell compartment and 23 subsets in the CD8⁺ T cell compartment (Figure 2A). Examples from a nasal polyp and a control sinus tissue are provided in Supplemental Figure E3. Comparison of multiple nasal polyps and control sinus tissues revealed two notable differences. First, naïve CD8⁺ T cells clustered into 5 subgroups based on CD127 (IL-7R), CXCR3, and CD161 expression (Figure 2A and 2B). Of these 5 subgroups, 4 were found in higher proportions in control nasal tissue than in nasal polyp tissues. One of those four, namely CD127^{hi}CXCR3^{hi}CD161^{lo}naïve CD8⁺ cells, was significantly more prevalent in control sinus tissue than nasal polyps ($p < 0.01$). Second, a subset of CD4⁺ T_{CM} cells, namely CD161^{hi}CXCR3^{lo}CD127^{lo}CD4⁺ T_{CM} cells, was present in 5 of 6 nasal polyp tissues, but was nearly absent in control sinus tissues (Figure 2A and 2C and Supplemental Figure E3). This subset of CD4⁺ T_{CM} cells expressed CCR7, CD28, CD45RO, CD69 and PD-1 but not CXCR5 or CD103 (Supplemental Figure E4A). Because antigen-specific CD161⁺ CD4⁺T cells vigorously produce IL-5 and IL-13 in response to allergen exposure⁷, this CD4⁺ T_{CM} subset may play a role in the pathophysiology of CRS and warrants further investigation in the future.

We used viSNE, an unsupervised algorithm that generates a 2-dimensional map of multi-dimensional data,⁸ to visualize mass cytometry T cell (CD45⁺CD3⁺CD19⁻cells) data (Figure 2D). Interestingly, a CD161^{hi}CXCR3^{lo}CD4⁺ T cell population (red box) similar to the CD161^{hi}CXCR3^{lo}CD127^{lo}CD4⁺ T_{CM} cells identified by the MDS map was detected via viSNE. By viSNE, the CD161^{hi}CXCR3^{lo}CD4⁺ population highly expressed CD69 and CD45RO but lacked CD127 or CD103, and was more frequent in nasal polyps than in control sinus tissues (Figure 2E, $p < 0.05$). Heat maps showed comparable molecular expression between CD161^{hi}CXCR3^{lo}CD127^{lo}CD4⁺ T_{CM} cells and CD161^{hi}CXCR3^{lo}CD4⁺ T cells identified by MDS map and viSNE, respectively (Supplemental Figure E4A and E4B). No other apparent differences in the CD4⁺ T cell subsets were detected between nasal polyps and control sinus tissues.

Finally, viSNE analysis of non-B, non-T cells (CD45⁺CD3⁻CD19⁻cells) revealed a distinct cell population found in nasal polyps, but not in control sinus tissues (Figure 2F, red circle). This innate cell population was positive for CD45RO, CD25, CRTH2, and CD69 and expressed low levels of CD127 and ST2 (the IL-33 receptor). Closer examination revealed variable expression of CD25, CRTH2, ST2 and CD127 within the population, suggesting that it may consist of several similar but heterogeneous cell types, including group 2 innate lymphoid cells (ILC2s)⁹. Further investigation, such as additional cell surface markers, gene expression and functional assays, will be necessary to elucidate the heterogeneity of this innate cell population and corresponding roles in nasal polyp pathobiology.

In summary, our study demonstrates that mass cytometry is comparable to flow cytometry for routine analysis while providing a robust capacity for identifying unique immune cell subsets in mucosal tissues through its high-dimensional resolution. However, several limitations must be considered. First, this study is preliminary due to its small sample size. As it was underpowered, likely several populations differentially

represented in nasal polyps versus control sinus tissues were missed. Second, in-depth analysis of cytokine and transcription factor expression and biologic functions of novel subsets, including naïve CD8⁺ cells, CD161^{hi}CD4⁺ T_{CM} cells, and ILC2-like cells, are warranted. Finally, it will be critical to compare nasal polyps from different CRS endotypes, such as aspirin-exacerbated respiratory disease, to fully decipher the T cell and lymphoid cell involvement in the disease process. Further studies using mass cytometry technology will provide an opportunity to make major progress in clinical studies in CRS and related disorders.

REFERENCES

1. Hopkins C. Chronic rhinosinusitis with nasal polyps. *N Engl J Med.* 2019; 381:55-63.
2. Stevens WW, Peters AT, Tan BK, Klingler AI, Poposki JA, Hulse KE, et al. Associations Between Inflammatory Endotypes and Clinical Presentations in Chronic Rhinosinusitis. *J Allergy Clin Immunol Pract* 2019; 7:2812-2820.
3. Hartmann FJ, Bendall SC. Immune monitoring using mass cytometry and related high-dimensional imaging approaches. *Nat Rev Rheumatol* 2020; 16:87-99.
4. Gebhardt T, Palendira U, Tschärke DC, Bedoui S. Tissue-resident memory T cells in tissue homeostasis, persistent infection, and cancer surveillance. *Immunol Rev.* 2018; 283:54-76.
5. Amir ED, Lee B, Badoual P, Gordon M, Guo XV, Merad M, et al. Development of a comprehensive antibody staining database using a standardized analytics pipeline. *Front Immunol* 2019; 10:1315.
6. Maecker HT, JP McCoy and R Nussenblatt. Standardizing immunophenotyping for the Human Immunology Project. *Nat Rev Immunol* 2012; 12:191.
7. Wambre E, Bajzik V, DeLong JH, O'Brien K, Nguyen QA, Speake C, et al. A phenotypically and functionally distinct human T_H2 cell subpopulation is associated with allergic disorders. *Sci Transl Med.* 2017; 9:eaam9171.
8. Amir ED, Davis KL, Tadmor MD, Simonds EF, Levine JH, Bendall SC, et al. viSNE enables visualization of high dimensional single-cell data and reveals phenotypic heterogeneity of leukemia. *Nat Biotechnol.* 2013; 31:545-52.
9. Liu S, Sirohi K, Verma M, McKay J, Michalec L, Sripada A, et al. Optimal identification of human conventional and nonconventional (CRTH2⁻IL7R α) ILC2s using additional surface markers. *J Allergy Clin Immunol.* 2020; 146:390-405.

AUTHORS

Kathleen R. Bartemes, PhD,^{1,2} Garret Choby, MD,² Erin K. O'Brien, MD,² Janalee K. Stokken, MD,² Kevin D. Pavelko, PhD,³ and Hirohito Kita, MD^{1,3,4}

¹Department of Allergic Diseases and Department of Medicine, ²Department of Otolaryngology, and ³Department of Immunology, Mayo Clinic, Rochester, MN, 55905, and ⁴Division of Allergy, Asthma, and Immunology and Department of Medicine, Mayo Clinic, Scottsdale, AZ 85259

ACKNOWLEDGEMENTS

This study was made possible through support of the Immune Monitoring Core, Mayo Clinic. The authors thank Kevin Brown, Ph.D., Fluidigm Corporation and El-ad David Amir, Ph.D., Astrolabe Diagnostics, for their expert assistance in panel design and data analysis and interpretation. This work was supported by grants from the National Institutes of Health (R01 HL117823, R37 AI71106) and the Mayo Foundation.

FIGURE LEGENDS

Figure 1. Flow cytometry and mass cytometry identify similar T cell subpopulations. (A) PBMCs and cells from control nasal tissues (Cont) and nasal polyps (NP) were stained for CD3⁺ T cell subsets using flow (left) or mass (right) cytometry. Ratios of CD4⁺ to CD8⁺ cell frequencies within the CD3⁺ T cell population are shown as means \pm SEMs. Flow cytometry, n=5 PBMC, 2 Cont, and 12 NP; Mass cytometry, n=3 PBMC, 2 Cont, and 6 NP. (B) CD3⁺ cells were analyzed biaxially for CD4⁺ and CD8⁺ expression. Flow (left) and mass (right) cytometry data are depicted as stacked means of CD4⁻CD8⁻ (double negative, DN), CD4⁺CD8⁺ (double positive, DP), CD4⁻CD8⁺ (CD8⁺) and CD4⁺CD8⁻(CD4⁺). (C) Proportions of

CD69⁺ cells within CD4⁺ T cells determined by flow (left) and mass (right) cytometry are shown as means \pm SEMs. Circles represent individual participants. (D) Proportions of CD69⁺ cells within CD8⁺ T cells determined by mass cytometry are shown as means \pm SEMs. Circles represent individual participants. (E and F) CD45⁺ leukocytes from mass cytometry data were clustered based on expression of canonical markers (see Supplemental Table E3 and Supplemental Figure E2). Frequency of naïve CD4⁺ and CD8⁺ T cells (Panel E) and CD8⁺ central memory T (T_{CM}) cells (Panel F) within the CD3⁺ population are shown as box and whisker plots. n=3 PBMC, 2 Cont, and 6 NP. *, p<0.05; **, p<0.01 between groups indicated by horizontal lines.

Figure 2. Identification of unique T cell and lymphoid cell populations in nasal polyps by mass cytometry. (A) MDS map of CD45⁺ leukocytes in nasal polyps after unsupervised clustering based on expression of surface markers. (B) Frequency of naïve CD8⁺ T cell subpopulations within CD3⁺ T cells in nasal polyps (NP) and control nasal tissues (Cont) is presented. (C) Frequency of the CD161^{hi}CXCR3^{lo}CD127^{lo}CD4⁺ T_{CM} population within CD3⁺ T cells in nasal polyps (NP) and control nasal tissues (Cont) is presented. ND, not detected. (D) viSNE mapping revealed clusters of T cell populations in CD45⁺CD3⁺CD19⁻ cells; representative nasal polyp (top) and control sinus tissue (bottom) are presented. Colors indicate marker expression levels as shown by the color key. Boxed cell population is unique to nasal polyps and minimally represented in control sinus tissues. (E) Frequency of a CD4⁺CD161^{hi}CXCR3^{lo} cell population (Panel D, boxed population) within CD45⁺CD3⁺CD19⁻ cells is shown. Each circle represents an individual subject. (F) viSNE mapping of CD45⁺CD3⁻CD19⁻ cells revealed a cluster of unique lymphoid cells (red circles) in nasal polyps but not in control sinus tissues; representative nasal polyp (top) and control sinus tissue (bottom) maps are presented. (G) Frequency of ILC2-like CD25⁺CRTH2⁺CD69⁺ cells (Panel F, circled population) within the CD45⁺CD3⁻CD19⁻ cell population is shown. Data in Panels B, C, E, and G are shown as means \pm SEMs. n=6 NP and n=2 Cont. *, p<0.05; **, p<0.01 between groups indicated by horizontal lines.

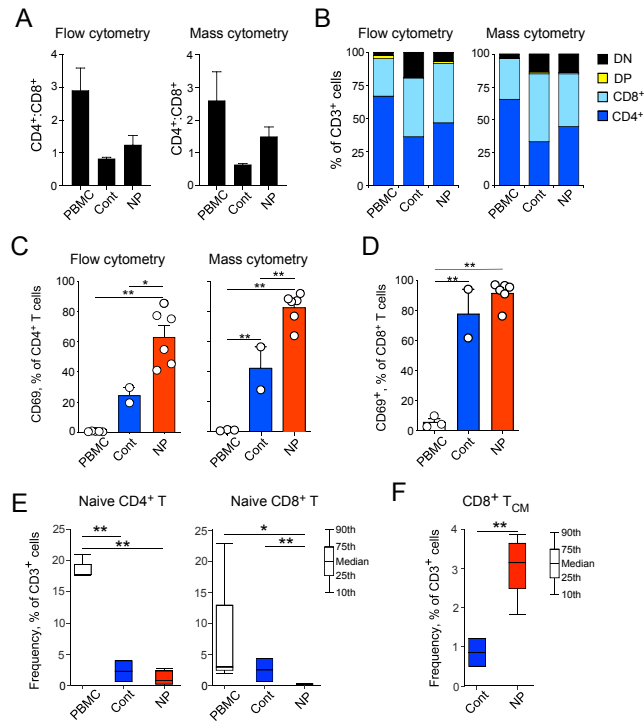


Figure 1

